



On the Pacific Decadal Oscillation and the Atlantic Multidecadal Oscillation: Might they be related?

Marc d'Orgeville¹ and W. Richard Peltier¹

Received 3 August 2007; revised 21 September 2007; accepted 1 November 2007; published 5 December 2007.

[1] The nature of the Pacific Decadal Oscillation (PDO) is investigated based upon analyses of sea surface temperature observations over the last century. The PDO is suggested to be comprised of a 20 year quasi-periodic oscillation and a lower frequency component with a characteristic timescale of 60 years. The 20 year quasi-periodic oscillation is clearly identified as a phase locked signal at the eastern boundary of the Pacific basin, which could be interpreted as the signature of an ocean basin mode. We demonstrate that the 60 year component of the PDO is strongly time-lag correlated with the Atlantic Multidecadal Oscillation (AMO). On this timescale the AMO is shown to lead the PDO by approximately 13 years or to lag the PDO by 17 years. This relation suggests that the AMO and the 60 year component of the PDO are signatures of the same oscillation cycle. **Citation:** d'Orgeville, M., and W. R. Peltier (2007), On the Pacific Decadal Oscillation and the Atlantic Multidecadal Oscillation: Might they be related?, *Geophys. Res. Lett.*, 34, L23705, doi:10.1029/2007GL031584.

1. Introduction

[2] Basin scale oceanic patterns of Sea Surface Temperature (SST) variability having timescales longer than inter-annual have been described in both northern oceans: these are the so-called Pacific Decadal Oscillation (PDO) [Mantua *et al.*, 1997] and the Atlantic Multidecadal Oscillation (AMO) [Kerr, 2000]. The explanations of these modes of climate variability continue to be debated but both appear to involve coupled ocean-atmosphere mechanisms. These climatic oscillations have therefore come to be investigated primarily through the use of coupled atmosphere-ocean global climate models (AOGCMs). In the current generation of such models, the spatial and temporal characteristics of these modes of variability are generally represented with acceptable accuracy. In statistically-equilibrated runs, both the PDO and the AMO appear as natural modes of variability of the climate system in their respective basins [Latif and Barnett, 1996; Delworth and Mann, 2000].

[3] This paper presents evidence, from an observational perspective, that the PDO and the AMO are strongly related to one another. The analyses presented herein are based upon the SST dataset provided by the Hadley Center (Met Office) [Rayner *et al.*, 2003], from which yearly, detrended and low pass filtered timeseries have been computed on a $1^\circ \times 1^\circ$ grid from 1870 to the present. The observational

data employed in this article as well as the methods we employ in their analysis are presented in the auxiliary material.¹

[4] Section 2 examines the PDO in some detail and suggests what appears to be a novel interpretation. Section 3 investigates the relationship between the PDO and the AMO. A summary of the results is presented in Section 4 together with a discussion of their consequences.

2. The PDO in Isolation

[5] The PDO is defined as the first Empirical Orthogonal Function (EOF) of SST anomalies above 20N in the Pacific basin (Figure 1a, EOF₁^{NP}, computed in the NP region: between 20N–65N and 120E–100W). In the North Pacific its pattern has a characteristic “horseshoe” shape, with opposite signs between the extremum in the central Pacific and that localized to the rim of the basin. Its time evolution, or Principal Component (Figure 1c, PC₁^{NP}), displays the characteristic decadal variability from which the mode derives its name. This decadal variability is superimposed on a lower frequency modulation, consisting of periods of stable sign separated by abrupt sign reversals as, for instance, in the case of the well known 1976/77 climate shift [Latif and Barnett, 1996].

[6] Even if the horseshoe pattern is now considered to be the classic signature of the PDO, its physics can probably not be captured by a single EOF. We therefore seek additional information on its nature through a combined study of the first two EOFs, which explain 34% and 30% of the variance respectively. The time-evolution of the second EOF, PC₂^{NP}, displays both decadal and multidecadal time scales, but with a more regular decadal oscillation than PC₁^{NP} (Figure 1c). Its spatial structure EOF₂^{NP} is primarily dominated by a strong extremum at the eastern boundary (Figure 1b).

[7] The EOF technique is an empirical mathematical framework that is often employed to decompose variability, but interpreting each EOF individually may be misleading. EOFs are orthogonal in time by construction, but can be physically related. The time-lag correlations between PC₁^{NP} and PC₂^{NP} reveal two extrema having values of 0.54 and -0.28 at lag -9 years and $+18$ years respectively. The same qualitative result holds if the analysis is done season by season instead of on the annually averaged data, even though the first two EOFs explain significantly different amounts of variance (for instance in winter with 41% and 21% for the first and second modes respectively).

[8] We have performed a continuous wavelet decomposition [Torrence and Compo, 1998] on both PC₁^{NP} and PC₂^{NP}.

¹Department of Physics, University of Toronto, Toronto, Ontario, Canada.

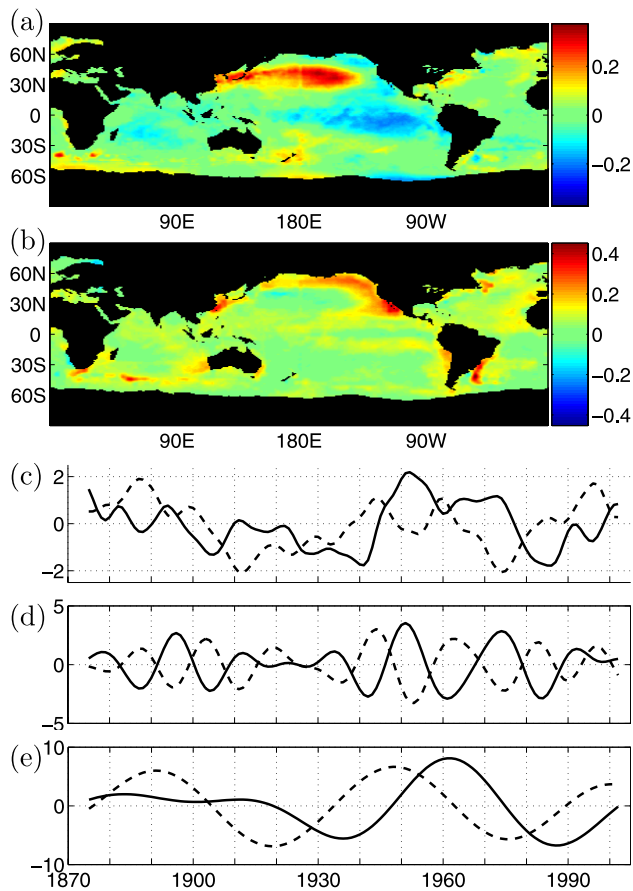


Figure 1. (a and b) First two EOFs (EOF_1^{NP} and EOF_2^{NP}) of SST anomalies for 1870 to present. (c) Corresponding principal components (PC_1^{NP} , solid; PC_2^{NP} , dashed) and their respective continuous wavelet transform coefficients for a (d) 20 year and (e) 60 year Morlet wavelet.

To restrict attention to frequencies that correspond to the same oscillation in both signals, time-lag correlations between same frequency components are computed for lags ranging between -30 and 30 years: if the same oscillation is present in both signals, the time-lag correlation as a function of the lag must exhibit a periodicity which corresponds to the pseudo period of the wavelet. From such an analysis (cf. auxiliary material) two frequencies dominate both signals and correspond approximately to periods of 20 and 60 years. These periods are approximate because the selected frequencies vary slightly depending on the nature of the wavelet employed. However their approximate values are believed to be reliable as these frequencies always correspond to extrema in the time-lag correlation among all frequencies independently of the wavelet type.

[9] The 60 year periodic components of PC_1^{NP} and PC_2^{NP} appear to be in phase quadrature (Figure 1d) and it will be shown in the next section that this 60 year period is connected to the variability of the Atlantic Ocean. The 20 year periodic components of PC_1^{NP} and PC_2^{NP} are out of phase (Figure 1e). This 20 year quasi-periodic variability is also evident in an oscillation in phase along the eastern boundary of the Pacific basin (Figure 2a).

[10] Apart from the tropical explanations of the PDO [Trenberth, 1990; Gu and Philander, 1997; Newman et al.,

2003], there are theories that also invoke the action of an extratropical mechanism acting alone. The SST variability has been suggested to be due to ocean adjustment through Rossby wave propagation, excited by stochastic atmospheric forcing [Frankignoul et al., 1997], with subsequent feedbacks of the ocean onto the atmosphere. Ocean-atmosphere coupling in the midlatitudes is unlikely to produce a new mode of variability but should be able to project modes of intrinsic ocean variability onto existing atmospheric modes of variability [Hogg et al., 2006]. In other words, the timescale and the physics of the coupled behaviour are likely to be controlled by ocean modes of variability, such as the classical ocean basin modes which are easily excited by atmospheric stochastic forcing [Cessi and Louazel, 2001] and by nonuniform forcing in the zonal direction [Pedlosky, 2006]. In some realistic AOGCMs, the PDO appears to evolve largely independently of the variations in the tropical Pacific and is rather controlled by the dynamical adjustment of the entire North Pacific ocean basin [Latif, 2006; Kwon and Deser, 2007]. In such models, the ocean basin modes are likely to be the driving mechanism of the simulated PDO.

[11] A fundamental characteristic of the ocean basin modes is their tendency to exhibit phase locking at the eastern boundary. This phase locking arises from the assumption of geostrophic motion which requires flat isopycnals at the eastern boundary [Cessi and Louazel, 2001]. Together with a global mass conservation constraint, this phase locking produces the coupling between the different latitudes, which is the basis for the existence of the ocean basin modes. In the case of excitation by stochastic atmospheric forcing, the frequency peak of the gravest ocean basin mode will therefore be more evident in a spectrum at the eastern boundary (spectra away from the eastern boundary have a complicated spatial dependence) [Cessi and Louazel, 2001]. In this context, the obvious 20 year periodic phased locked signal at the eastern boundary (Figure 2a) can be interpreted as primary evidence of the importance of ocean basin modes in the physics of the PDO.

[12] Moreover, for a given basin, another fundamental characteristic of ocean basin modes is that the period of the

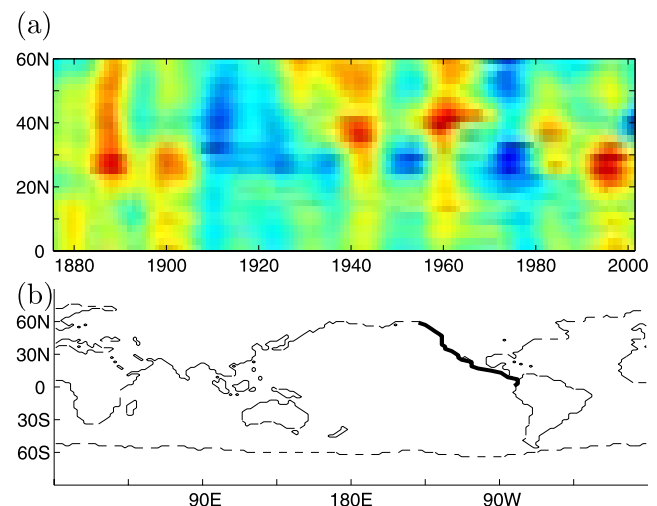


Figure 2. (a) Time-latitude diagram of SST anomalies along the eastern boundary, defined in (b).

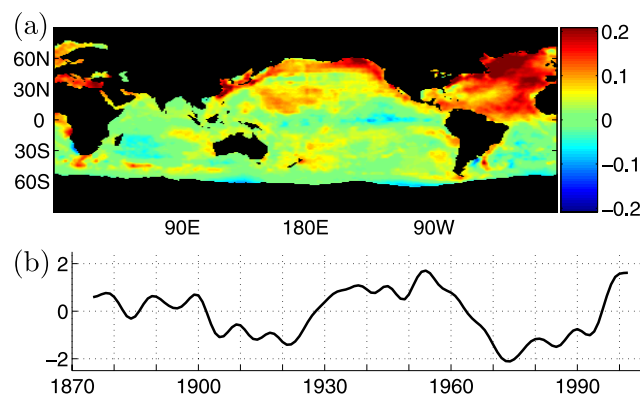


Figure 3. (a) AMO structure as the first EOFs of SST anomalies in the North Atlantic (EOF^{NA}) for 1870 to present (maximum of 0.4°C in the NA region). (b) AMO index defined as the corresponding principal component (PC^{NA}).

gravest mode is fixed by the longest transit time of long Rossby waves between the eastern and western boundaries [Cessi and Louazel, 2001]. Zonal propagation has already been recognized in subsurface temperatures [Zhang and Levitus, 1997], and with the filtering employed in the present study, the available time series of SST anomalies do enable the visualization of westward propagating signals at different latitudes (Figure S1, auxiliary material). The phase speed, that can be inferred from SST signals, decreases with latitude, but because of the decreasing width of the basin with latitude, the transit time is of the same order of magnitude for all latitudes, varying from approximately 10 years in low latitude to 20 years in midlatitude (Figure S1). At 40°N , standing oscillations can also be detected, which would mean that advection by the gyre circulation is not negligible for such basin scale modes [Latif and Barnett, 1996; Ben Jelloul and Huck, 2005].

[13] The phase locking at the eastern boundary, together with the inferred westward zonal propagation, are strong indications that the decadal part of the PDO can be explained in terms of ocean basin modes. These two signatures of the basin adjustment process both suggest a period of approximately 20 years.

[14] Based upon our analysis of observed SSTs, the North Pacific variability may therefore be interpreted as consisting of a superposition of decadal timescale ocean basin modes and lower frequency variability having a multidecadal timescale.

3. The PDO and the AMO: Interconnections

[15] The AMO is a coherent pattern of multidecadal variability in sea surface temperature centred on the North Atlantic Ocean. The most likely explanation of the AMO has been suggested to involve an oceanic mode of variability connected to the thermohaline circulation [Delworth and Mann, 2000; Knight et al., 2005; Justino and Peltier, 2005]. The AMO may be defined as the first EOF of SST anomalies in the North Atlantic region (NA, between 20°N – 65°N and 100°W – 0°E), which explains 50% of the variance (Figure 3a, EOF^{NA}). In the 130 year duration of the dataset, its associated time series (Figure 3b, PC^{NA}) clearly displays two periods of oscillation, with the ampli-

tude being larger for the second and longer period. Decadal timescale variability also seems to be superimposed upon this low-frequency structure but this is not as important as was shown to be the case for the PDO in the previous Section.

[16] The spatial pattern of the AMO (EOF^{NA} , Figure 3a), is characterized by a constant sign in the entire North Atlantic basin and tends to exhibit the same sign almost everywhere, except in the South Atlantic and in the equatorial Pacific. In this regard, and also as a consequence of the existence of an extremum near the eastern boundary of the North Pacific basin, EOF^{NA} resembles EOF_2^{NP} . In fact, the spatial correlation of EOF_2^{NP} and EOF^{NA} is 0.87 in the NA region and 0.73 in the NP region, but the relative difference in amplitude in each basin masks these correlations. Their corresponding time series, PC^{NA} and PC_2^{NP} , however, are only weakly correlated because of the dominance of multidecadal time scales in the former and decadal time scales in the latter. Based upon the EOF decompositions alone, the link between the AMO and the PDO, though intuitively appealing, is not at all obvious.

[17] In order to more sharply focus upon the multidecadal time scale of the AMO and to more directly seek to describe its connection to Pacific variability, regressions on the AMO index (defined here as PC^{NA}) have been computed for different assumed time lags. The computed spatial patterns from these time-lag regressions are then compared with the PDO pattern (defined as EOF_1^{NP}): their spatial correlation in the NP area has a maximum value of 0.95 at 13 year lag and a minimum value of -0.93 at -17 year lag (Figure 4a, solid line). The spatial correlations of the global patterns reveal approximately the same extrema (Figure 4a, dashed line, $0.92/13$ years and $-0.86/-19$ years). These very large spatial correlations are the signature of the strong link between the multidecadal variability of the PDO and the AMO. But since the amplitude of both the 13 year lag regression pattern and the PDO pattern are of the same order of magnitude in the NP area (Figure 4b and Figure 1a), this does not provide any indication concerning which of the PDO or the AMO should be considered the leading signal.

[18] The PDO index (defined as PC_1^{NP}) is also strongly time-lag correlated with the AMO index with approximately the same lags (Figure 4a, thin line, $0.69/13$ years and $-0.67/$

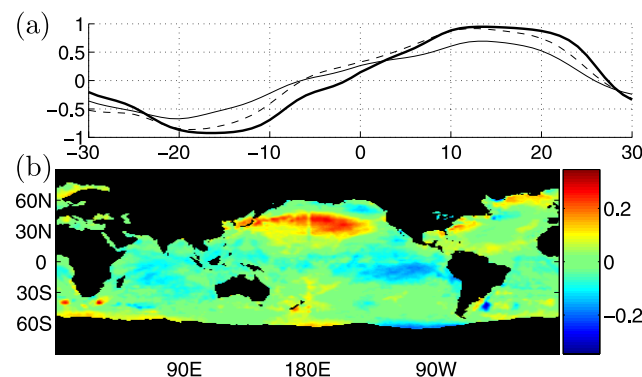


Figure 4. (a) Spatial correlation between the PDO and the time-lag regression on the AMO index. (b) Spatial structure of the time-lag correlation on the AMO index at lag 13 years.

–20 years). The fact that in these time-lag correlation curves, two extrema of opposite sign exist at two lags of opposite sign is reminiscent of two components in phase quadrature of a unique oscillation cycle. Nevertheless, both AMO and PDO related time-series are intrinsically dependent on the definition of their spatial pattern, making interpretation of their phase relationship challenging.

[19] Finally, significance tests have been computed from 10000 red noise time series with the same lag-1 year autocorrelation as the AMO index. These synthetic time series have been low-pass filtered and then regressed onto the SST field for different time-lags. In spite of smoothing and the shortness of the observational record used, all the time-lag correlation extrema of Figure 4a are above the 95% significance level, with the positive maxima exceeding the 99% level.

4. Discussion

[20] It has been argued that the Pacific Decadal Oscillation (PDO) may be viewed as comprising decadal timescale basin modes of ocean adjustment, superimposed upon a multidecadal modulation. This lower frequency component has been shown to be the signature in the North Pacific ocean of the Atlantic Multidecadal Oscillation (AMO). The AMO leads the PDO by 13 years or lags the PDO by 17 years. Both the AMO and the low frequency component of the PDO appear to be part of the same 60 year oscillation cycle.

[21] One possible explanation is that the two basins are collectively involved in producing variability on a timescale of 60 years, with teleconnections acting in both directions, the AMO and the low frequency component of the PDO being two components in phase quadrature of the same oscillation cycle. On the other hand, the 60 year timescale of the AMO could arise as a consequence of the natural multidecadal variability of the thermohaline circulation in the Atlantic basin alone [Delworth and Mann, 2000; Justino and Peltier, 2005]. In this most plausible interpretation, the AMO-alone affects the global Northern hemisphere atmospheric circulation which subsequently triggers an adjustment of the Pacific Ocean circulation. Local air-sea interaction feedback in the Pacific could be involved in determining the timelag of this adjustment process, as recently alluded to by [Zhang and Delworth, 2007] based upon results obtained using a hybrid coupled model.

[22] The characteristic timescales of the PDO (20 and 60 years) and the AMO (60 years) have also been detected in tree ring chronologies extending over the last 3 centuries [Minobe, 1997; Biondi et al., 2001; Gray et al., 2004]. However such reconstructions do not provide the corresponding SST patterns, and therefore it is not possible using them to assess whether the PDO and AMO were similarly related before the 20th century. Rather, the relation between the PDO and the AMO may be studied only over the last century as we have done here.

[23] For this period, during which Global Warming is also recognised to be acting, there is, not unreasonably, an ongoing debate as to what fraction of the AMO might be due to natural variability as opposed to being directly forced by Global Warming [Trenberth and Shea, 2006; Zhang et al., 2007]. We are therefore obliged to question whether the

relation between the PDO and the AMO discussed herein could be a direct response to the anthropogenic forcing. If this was the case, it could help to explain why a change in the PDO period over the last century has been inferred on the basis of tree ring chronologies [Biondi et al., 2001].

[24] Because of the shortness of the observed SST reconstructions (130 years) compared to the multidecadal timescale studied herein (60 years), from a statistical point of view there is a clear need for appropriate AOGCM simulations that are able to reproduce the common multidecadal variability. Preliminary results obtained from such statistical equilibrium simulations demonstrate that a common multidecadal mode of variability between the Pacific and Atlantic basins does indeed exist. Such preliminary results provide some confidence concerning the existence of a PDO-AMO relation revealed by the analysis of the observations presented herein. A complete discussion of the results obtained in an ensemble of such simulations will be reported elsewhere.

[25] **Acknowledgments.** This letter is a contribution to the Polar Climate Stability Network which is sponsored by the Canadian Foundation for Climate and Atmospheric Sciences and a Consortium of Canadian Universities. Additional support has been provided by NSERC Discovery grant A9627. The authors would like to thank two anonymous reviewers for their valuable comments which helped to improve the manuscript.

References

- Ben Jelloul, M., and T. Huck (2005), Low-frequency basin modes in a two-layer quasigeostrophic model in the presence of a mean gyre flow, *J. Phys. Oceanogr.*, *35*, 2167–2186.
- Biondi, F., A. Gershunov, and D. R. Cayan (2001), North Pacific decadal variability since 1661, *J. Clim.*, *14*, 5–10.
- Cessi, P., and S. Louazel (2001), Decadal oceanic response to stochastic wind forcing, *J. Phys. Oceanogr.*, *31*, 3020–3029.
- Delworth, T. L., and M. E. Mann (2000), Observed and simulated multidecadal variability in the Northern Hemisphere, *Clim. Dyn.*, *16*, 661–676.
- Frankignoul, C., P. Muller, and E. Zoritta (1997), A simple model of the decadal response of the ocean to stochastic forcing, *J. Phys. Oceanogr.*, *27*, 1533–1546.
- Gray, S. T., L. J. Graumlich, J. L. Betancourt, and G. T. Pederson (2004), A tree-ring based reconstruction of the Atlantic Multidecadal Oscillation since 1567 A.D., *Geophys. Res. Lett.*, *31*, L12205, doi:10.1029/2004GL019932.
- Gu, D., and S. G. H. Philander (1997), Interdecadal climate fluctuations that depend on exchanges between the tropics and extratropics, *Science*, *275*, 805–807.
- Hogg, A. M., W. K. Dewar, P. D. Killworth, and J. R. Blundell (2006), Decadal variability of the midlatitude climate system driven by the ocean circulation, *J. Clim.*, *19*, 1149–1166.
- Justino, F., and W. R. Peltier (2005), The glacial North Atlantic Oscillation, *Geophys. Res. Lett.*, *32*, L21803, doi:10.1029/2005GL023822.
- Kerr, R. (2000), A North Atlantic climate pacemaker for the centuries, *Science*, *288*, 1984–1986.
- Knight, J. R., R. J. Allan, C. K. Folland, M. Vellinga, and M. E. Mann (2005), A signature of persistent natural thermohaline circulation cycles in observed climate, *Geophys. Res. Lett.*, *32*, L20708, doi:10.1029/2005GL024233.
- Kwon, Y.-O., and C. Deser (2007), North Pacific decadal variability in the Community Climate System Model version 2, *J. Clim.*, *20*, 2416–2433.
- Latif, M. (2006), On North Pacific multidecadal climate variability, *J. Clim.*, *19*, 2906–2915.
- Latif, M., and T. P. Barnett (1996), Decadal variability over the North Pacific and North America: Dynamics and predictability, *J. Clim.*, *9*, 2407–2423.
- Mantua, N. J., S. R. Hare, Y. Zhang, J. M. Wallace, and R. C. Francis (1997), A Pacific interdecadal climate oscillation with impacts on salmon production, *Bull. Am. Meteorol. Soc.*, *78*, 1069–1079.
- Minobe, S. (1997), A 50–70 year climatic oscillation over the North Pacific and North America, *Geophys. Res. Lett.*, *24*, 683–686.
- Newman, M., G. P. Combo, and M. A. Alexander (2003), ENSO-forced variability of the Pacific Decadal Oscillation, *J. Clim.*, *16*, 3853–3857.

- Pedlosky, J. (2006), Time-dependent response to cooling in a beta-plane basin, *J. Phys. Oceanogr.*, *36*, 2186–2198.
- Rayner, N. A., D. E. Parker, E. B. Horton, C. K. Folland, L. V. Alexander, D. P. Rowell, E. C. Kent, and A. Kaplan (2003), Global analyses of sea surface temperature, sea ice, and night marine air temperature since the late nineteenth century, *J. Geophys. Res.*, *108*(D14), 4407, doi:10.1029/2002JD002670.
- Torrence, C., and G. P. Compo (1998), A practical guide to wavelet analysis, *Bull. Am. Meteorol. Soc.*, *79*, 61–78.
- Trenberth, K. E. (1990), Recent observed interdecadal climate changes in the Northern Hemisphere, *Bull. Am. Meteorol. Soc.*, *71*, 988–993.
- Trenberth, K. E., and D. J. Shea (2006), Atlantic hurricanes and natural variability in 2005, *Geophys. Res. Lett.*, *33*, L12704, doi:10.1029/2006GL026894.
- Zhang, R., and T. L. Delworth (2007), Influence of the Atlantic Ocean on the Northern Pacific multidecadal climate variability, *Geophys. Res. Abstr.*, *9*, 11210, sref:1607-7962/gra/EGU2007-A-11210.
- Zhang, R., T. L. Delworth, and I. M. Held (2007), Can the Atlantic Ocean drive the observed multidecadal variability in Northern Hemisphere mean temperature?, *Geophys. Res. Lett.*, *34*, L02709, doi:10.1029/2006GL028683.
- Zhang, R.-H., and S. Levitus (1997), Structure and cycle of decadal variability of upper-ocean temperature in the North Pacific, *J. Clim.*, *10*, 710–727.

M. d'Orgeville and W. R. Peltier, University of Toronto, 60 St. George Street, Toronto, ON, Canada M5S 1A7. (marcdo@atmosph.physics.utoronto.ca)